

Endothelial Immune Activation by Medin: Potential Role in Cerebrovascular Disease and Reversal by Monosialoganglioside-Containing Nanoliposomes

Nina Karamanova, DVM; Seth Truran, BS; Geidy E. Serrano, PhD; Thomas G. Beach, MD; Jillian Madine, PhD; Volkmar Weissig, PhD; Hannah A. Davies, PhD; Jaimeson Veldhuizen, BS; Mehdi Nikkhah, PhD; Michael Hansen, BS; Weiyang Zhang, PhD; Karen D'Souza, PhD; Daniel A. Franco, PhD; Raymond Q. Migrino, MD

Background—The function of medin, one of the most common human amyloid proteins that accumulates in the vasculature with aging, remains unknown. We aim to probe medin's role in cerebrovascular disease by comparing cerebral arterial medin content between cognitively normal and vascular dementia (VaD) patients and studying its effects on endothelial cell (EC) immune activation and neuroinflammation. We also tested whether monosialoganglioside-containing nanoliposomes could reverse medin's adverse effects.

Methods and Results—Cerebral artery medin and astrocyte activation were measured and compared between VaD and cognitively normal elderly brain donors. ECs were exposed to physiologic dose of medin (5 $\mu\text{mol/L}$), and viability and immune activation (interleukin-8, interleukin-6, intercellular adhesion molecule-1, and plasminogen activator inhibitor-1) were measured without or with monosialoganglioside-containing nanoliposomes (300 $\mu\text{g/mL}$). Astrocytes were exposed to vehicle, medin, medin-treated ECs, or their conditioned media, and interleukin-8 production was compared. Cerebral collateral arterial and parenchymal arteriole medin, white matter lesion scores, and astrocyte activation were higher in VaD versus cognitively normal donors. Medin induced EC immune activation (increased interleukin-8, interleukin-6, intercellular adhesion molecule-1, and plasminogen activator inhibitor-1) and reduced EC viability, which were reversed by monosialoganglioside-containing nanoliposomes. Interleukin-8 production was augmented when astrocytes were exposed to medin-treated ECs or their conditioned media.

Conclusions—Cerebral arterial medin is higher in VaD compared with cognitively normal patients. Medin induces EC immune activation that modulates astrocyte activation, and its effects are reversed by monosialoganglioside-containing nanoliposomes. Medin is a candidate novel risk factor for aging-related cerebrovascular disease and VaD. (*J Am Heart Assoc.* 2020;9:e014810. DOI: 10.1161/JAHA.119.014810.)

Key Words: aging • amyloid • cerebrovascular disease • inflammation • vascular dementia

Age is the most important risk factor for cerebrovascular disease (CVD) and cognitive dysfunction disorders, including vascular dementia (VaD).¹ Even in the absence of traditional cardiovascular risk factors, aging results in well-defined vascular phenotypic changes, including endothelial dysfunction² and chronic indolent low-grade inflammation, leading to atherosclerosis and CVD.³ Although the molecular, functional, and structural changes of aging-related CVD have

been documented,³ the specific intrinsic biologic determinants of these changes remain largely unknown. Medin, a 50–amino acid peptide, forms one of the most common types of human amyloid^{4,5} and accumulates in the vasculature with aging,^{6–9} yet its biologic effects are still largely unknown. It is a cleavage product from parent protein milk fat globule–EGF factor 8 protein.⁴ It is widely known to be present in aging aorta,⁴ with little to no aortic medin in patients aged

From the Phoenix Veterans Affairs, Phoenix, AZ (N.K., S.T., M.N., M.H., W.Z., K.D., D.A.F., R.Q.M.); Banner Sun Health Research Institute, Sun City, AZ (G.E.S., T.G.B.); University of Liverpool, United Kingdom (J.M., H.A.D.); Midwestern University, Glendale, AZ (V.W.); Arizona State University, Tempe, AZ (J.V., M.N.); and University of Arizona College of Medicine–Phoenix, Phoenix, AZ (R.Q.M.).

Accompanying Figures S1 through S4 are available at <https://www.ahajournals.org/doi/suppl/10.1161/JAHA.119.014810>

Correspondence to: Raymond Q. Migrino, MD, Phoenix Veterans Affairs Health Care System, 650 E Indian School Rd, Phoenix, AZ 85022. E-mail: raymond.migrino@va.gov

Received September 30, 2019; accepted December 4, 2019.

© 2020 The Authors. Published on behalf of the American Heart Association, Inc., by Wiley. This is an open access article under the terms of the Creative Commons Attribution-NonCommercial-NoDerivs License, which permits use and distribution in any medium, provided the original work is properly cited, the use is non-commercial and no modifications or adaptations are made.

Clinical Perspective

What Is New?

- Medin is one of the most common aging-related amyloid proteins whose function is largely unknown; the study shows increased cerebral artery medin and astrocyte activation in elderly brain donors with vascular dementia compared with those who are cognitively normal.
- In vitro experiments show medin inducing immune activation in endothelial cells that modulate astrocyte activation and that these effects are reversed by monosialoganglioside-containing nanoliposomes through nuclear factor erythroid 2-related factor 2-dependent antioxidant pathway.

What Are the Clinical Implications?

- The findings point to the potential role of medin in cerebrovascular inflammation, leading to neuroinflammation that could be a novel biologic mechanism and treatment target for vascular dementia and vascular aging.
- The study also points to nanoliposomes as potential novel therapeutic approach for medin-induced vasculopathy.

<55 years and increased aortic medin in those aged ≥ 55 years,⁶ but the extent or degree of accumulation in cerebral vessels has not been reported. We previously reported that treatment with physiologic doses of medin induced endothelial dysfunction in human peripheral and cerebral arterioles, mediated by oxidative and nitrative stress.^{6,10} We also showed initial observations that medin increased proinflammatory cytokine production by endothelial cells (ECs). These findings support the potential role of medin as a novel agent in vascular aging pathological characteristics, leading to CVD. Furthermore, medin's effect on the vasculature could potentially influence the perivascular milieu. In VaD, neuroinflammation occurs proximate to cerebral arterioles. Activated astrocytes and microglia, cellular markers of neuroinflammation, are commonly found in regions of white matter changes¹¹ concentrating around blood vessels.¹² This suggests tight vasculoneural inflammatory coupling. Cerebral white matter lesions (CWMLs) in aging and neurodegenerative diseases, such as VaD, represent microvascular ischemic changes associated with both endothelial and glial activation¹³ that are highly associated with dementia and stroke.¹⁴ Neuroinflammation by itself can contribute to neurodegeneration and cognitive dysfunction in VaD and Alzheimer disease.^{12,15} Therefore, the initiation or aggravation of neuroinflammation by vascular inflammation could be one of the critical mechanisms explaining the tight link among aging, CVD, and dementia disorders. We aimed to probe medin's role in CVD by comparing cerebral arteriole medin content between cognitively normal (CN) and VaD patients and

studying its effects on EC immune activation and modulation of neuroinflammation. Herein, we define EC immune activation as induction of EC production of proinflammatory cytokines or chemokines after exposure to an agent, similar to previous studies.^{16–18}

We likewise previously showed that nanoliposomes (artificial phospholipid vesicles <100 nm in diameter) that contain monosialogangliosides (NLGM1) or phosphatidic acid prevented endothelial dysfunction induced by other amyloid proteins, specifically AL amyloid light chain proteins¹⁹ or β -amyloid,²⁰ respectively. We also tested whether NLGM1 could reverse medin's adverse effects while identifying potential mechanisms for the protection.

Methods

The data that support the findings of this study are available from the corresponding author on reasonable request.

Medin and NLGM1

Recombinant medin was used for treatment conditions in the study. Medin was expressed in Lemo 21 (DE3) cells using pOPINS-medin, and details of its preparation and purification can be found in prior work.^{6,16} Medin was confirmed to have >95% purity by SDS-PAGE and characterized by matrix-assisted laser desorption as well as ionization mass spectrometry. Endotoxin levels were confirmed to be <0.5 ng/mL using *Limulus* Amebocyte Lysate assay (Pierce, Dallas, TX).

NLGM1 was prepared from phosphatidylcholine, cholesterol, and monosialoganglioside (molar ratios, 70:25:5) using lipid film hydration method, details of which have been published.¹⁴ Lipid components were dissolved in chloroform, and the solvent was removed by drying in a rotary vacuum evaporator until a thin lipid film was formed. This lipid film was hydrated with HEPES solution (pH 7.4) to obtain a final lipid concentration of 10 mg/mL. This liposomal suspension was sonicated for 45 minutes (Sonic Dismembrator Model 100; Fisher Scientific) in an ice bath until an opaque solution was formed, which indicates the formation of small unilamellar vesicles (nanoliposomes). To precipitate and remove titanium particles sloughed off from the probe during sonication, NLGM1 was centrifuged at 101g for 15 minutes at 4°C.

Brain Tissue Sources, Western Blot, and Histopathology

Donors gave informed consent for postmortem brain donation under the Brain and Body Donation Program.²¹ The program's operations have been approved by the Banner Sun Health Research Institute Institutional Review Board. In a first group

of donors, cerebral collateral arteries (diameter range ≈ 100 – $2200 \mu\text{m}$) from CN and VaD participants were isolated from leptomeninges after rapid autopsy (postmortem interval, 3.4 ± 0.2 hours). VaD diagnosis was adjudicated by an expert neuropathologist (T.G.B.) using National Institute of Neurological Disorders and Stroke and Association Internationale pour la Recherche et l'Enseignement en Neurosciences (NIND-AIRENS) criteria.²² CN was the diagnosis if there was no cognitive dysfunction and if there was only age-consistent neuropathology.²¹ Tissue handling details were reported previously.⁶ In brief, tissues were immediately placed in sterile HEPES buffer (4°C ; pH 7.4). Arteries were isolated and homogenized in tissue lysis buffer (radioimmunoprecipitation assay or tris-buffered saline–Triton X-100 1%). Tissue samples ($60 \mu\text{g}$ of protein, determined by Bradford assay) and recombinant medin (0.01, 0.1, or $0.5 \mu\text{g}$) were loaded for electrophoresis, and Western blot was performed as previously detailed.²³ Primary antibody against medin (18G1; 1:500; generously provided by Prothena Biosciences Limited, Dublin, Ireland) and 800CW (800 nm) infrared fluorescent conjugated goat secondary antibody (Li-COR Biosciences, Lincoln, NE) were used. Bands were detected using Li-COR Odyssey CLx system (Image Studio 4.0) and normalized to β -actin loading control. A standard curve was plotted using the medin samples and used to calculate tissue medin content.

CWMLs are known to be caused by cerebral small-vessel disease and are important in the pathophysiological characteristics of VaD and other dementia disorders.²⁴ The brain sources of cerebral collateral arteries were scored (G.S. and T.G.B.) for CWML using 4% formaldehyde-treated tissue slices, as detailed in previously published work.²⁵ In brief, a score of 1 denotes CWMLs restricted to the immediate periventricular area, occupying less than a third of the centrum semiovale; 2, involvement of one third to two thirds of the centrum semiovale; and 3, involvement of more than two thirds of the centrum semiovale. The scores in the frontal, temporal, parietal, and occipital regions were added to obtain the CWML total score and compared between CN and VaD donors. Arteriole medin content was also compared between donors with high (median value or greater) versus low (less than median value) CWML scores.

In a separate second group of donors with banked brain tissue but without available leptomeningeal tissue, paraformaldehyde-treated, paraffin-embedded middle frontal gyrus tissues from CN and VaD donors ($5 \mu\text{m}$ sections) were analyzed. Astrocyte activation was assessed by immunohistochemistry using anti-GFAP (glial fibrillary acidic protein) primary antibody (1:150; Cell Signaling Technology), horseradish peroxidase-conjugated secondary antibody, and 3,3-diaminobenzidine staining and costained with hematoxylin-eosin. Imaging was performed on a Biotek Cytation 5 (Winooski, VT), and 3,3-diaminobenzidine-positive cells were

manually counted from 5 areas uniformly spaced around a central beacon set by operator. In randomly selected CN and VaD donors ($N=3$ each), GFAP-expressing astrocytes were counted ≤ 100 and $> 100 \mu\text{m}$ from cerebral arterioles. In next adjacent $5\text{-}\mu\text{m}$ tissue sections, parenchymal cerebral arteriole medin was assessed by immunohistochemistry using anti-medin antibody (1:1000) and 3,3-diaminobenzidine staining was assessed with 3,3-diaminobenzidine-positive wall area (expressed as percentage of arteriole wall area), quantified using Gen5 Image Plus Version 3.03.14 software (Biotek). For figure illustration purposes, costaining with anti-GFAP using fluorescent secondary antibody (IRDye 680RD; LiCOR Inc, Lincoln, NE) and Hoechst 33258 (Sigma-Aldrich, St Louis, MO) nuclear staining were performed.

EC Immune Activation

Primary culture human umbilical vein ECs (passages 4–8; Lonza, Walkersville, MD) were seeded into 6-well plates and grown to full confluence. Human umbilical vein ECs have been extensively used to study vascular cell behavior in neurodegenerative disease studies, such as Alzheimer disease and VaD, as they show similarity in properties as brain ECs, including $A\beta$ metabolism,^{26,27} expression of tight junction proteins,²⁸ and metabolic interactions with neural cells.²⁹ ECs were exposed to 20 hours of vehicle or medin ($5 \mu\text{mol/L}$; dose chosen as this was the mean medin concentration found in human vascular tissue⁶) without or with NLGM1 ($300 \mu\text{g/mL}$). Additional replicates were also treated with NLGM1 ($300 \mu\text{g/mL}$) plus transcription factor nuclear factor erythroid 2-related factor 2 (Nrf2) inhibitor brusatol ($1 \mu\text{mol/L}$). EC immune activation was assessed using gene and protein expressions of inflammation-related cytokines/chemokines interleukin-8, interleukin-6, intercellular adhesion molecule (ICAM)-1, and plasminogen activator inhibitor (PAI)-1 (all primers from IDT DNA Technologies, Coralville, IL); method details were reported.^{6,19} After lysis, RNA was extracted and converted to cDNA using Aurum Total RNA Mini Kit and iScript cDNA synthesis kit (Bio-Rad Laboratories, Coralville, IA) with β -actin as reference normalization gene. We previously showed that medin-induced increases in EC interleukin-8 and interleukin-6 were nuclear factor- κB (NF κB) mediated⁶, and to confirm whether effects on ICAM-1 and PAI-1 were also NF κB mediated, we also cotreated medin with a specific small-molecule inhibitor of NF κB ,³⁰ RO106-9920 ($100 \mu\text{mol/L}$; Tocris Biosciences, Bristol, UK), in additional replicates.

The conditioned cell media from treated ECs were analyzed for interleukin-8 and interleukin-6 protein by ELISA using DuoSet kit (R&D Systems, Minneapolis, MN). ICAM-1 protein was measured from whole cell lysate using ICAM-1 ELISA kit (R&D Systems). PAI-1 and phosphorylated NF κB (Ser536;

93H1) proteins were measured using Western blot (1:500; Cell Signaling Technology, Danvers, MA).

To assess effects of medin on immune activation of human brain microvascular ECs, human brain microvascular ECs (passages 3–5; Lonza) were exposed for 20 hours to vehicle or medin (5 $\mu\text{mol/L}$), and gene expression levels of interleukin-8, interleukin-6, and ICAM-1 were compared.

EC Viability and Oxidative Stress

Treated ECs were incubated (15 minutes) with dihydroethidium (5 $\mu\text{mol/L}$; Molecular Probes) to assess superoxide,³¹ calcein-acetoxymethyl (10 nmol/L ; Life Technologies),³² annexin V–fluorescein isothiocyanate (0.5 $\mu\text{g/mL}$; eBiosciences, San Diego, CA), or propidium iodide (0.15 $\mu\text{mol/L}$; Sigma-Aldrich)³³ to assess cell viability using flow cytometer (FC500; Beckman Coulter, Indianapolis, IN) at the following excitation/emission settings: 490/626 nm (dihydroethidium), 494/517 nm (calcein-acetoxymethyl), 488/525 nm (annexin V), and 488/620 nm (propidium iodide). Compensation adjustment was made to aid the classification of cellular populations and minimize cross-channel contamination, and the compensation setting was applied uniformly to all the assays.

Activated Nrf-2 protein was measured by separating the nuclear from cytosolic components using NE-PER Nuclear and Cytoplasmic Extraction kit (Thermo Scientific, Rockford, IL) and using anti-Nrf2 primary antibody (1:500; Cell Signaling) on nuclear proteins using Western blot with tubulin as loading control. Heme oxygenase (HO)-1 and NAD(P)H quinone dehydrogenase 1 (NQO1) proteins were measured from whole cell lysates using anti-HO-1 (1:1000; Cell Signaling Technology) and anti-NQO1 (1:1000; Cell Signaling) primary antibodies. Gene expression levels of HO-1, NQO1, and superoxide dismutase-1 (SOD1) were measured using primers from IDT DNA Technologies, similar to methods described above.

Astrocyte Monoculture

Human primary astrocytes (passage 3; Gibco, Madison, WI) were seeded in gelatin matrix (4×10^4 cells/cm²) coated plates, grown in astrocyte culture media, and allowed to attach overnight. The media were then changed with 1 of 4 different conditions: (1) 100% astrocyte media (vehicle), (2) 100% astrocyte media with 5 $\mu\text{mol/L}$ medin, (3) 90% astrocyte media and 10% conditioned media from ECs grown in EC media, or (4) 90% astrocyte media and 10% conditioned media from ECs treated for 20 hours with 5 $\mu\text{mol/L}$ medin (schema summarized in Figure S1). After 20 hours, astrocyte-conditioned media were collected and interleukin-8 was measured by ELISA; values reported represent interleukin-8 produced solely by astrocytes (measured interleukin-8 minus interleukin-8 content from EC culture media treatment). To

assess whether EC media affect astrocyte interleukin-8 production, we separately measured interleukin-8 in conditioned media of astrocytes grown in astrocyte media and astrocytes exposed to 90%/10% astrocyte/EC media for 20 hours and found no significant difference in interleukin-8 production (42.1 ± 23.6 versus 38.0 ± 18.7 pg/mL, respectively; $N=3$; $P=0.6$).

Microfluidic Chip Fabrication and 3-Dimensional Chip Astrocyte and EC Coculture

The microfluidic platform was fabricated in polydimethylsiloxane using standard SU-8 photolithography and replica molding technique, consistent with our earlier work.^{34–36} The platform consisted of 2 side channels for seeding of ECs and a central region for astrocyte culture. The dimensions of the side channels' length, width, and height are 4 mm, 250 μm , and 200 μm , respectively. The width of the 3-dimensional central region is 2 mm. Elliptical microposts were localized within the central tissue region (500- μm width, 100- μm height) with specific micropost spacing to optimize alignment of the astrocytes, while maintaining cellular connectivity and paracrine signaling. Creation of the master silicon wafer through photolithography was executed through spin coating of SU-8 on a wafer to a height of 200 μm . The wafer was soft baked, then exposed to UV through a transparent photomask with the chip design. After postbaking, the developed wafer was used as the substrate for soft lithography with polydimethylsiloxane replica molding. A polydimethylsiloxane base:curing agent ratio of 10:1 was used. Then, the polydimethylsiloxane channels were bonded to glass slides through oxygen plasma. The polydimethylsiloxane-glass bonded device was sterilized through autoclave, and subsequently the main tissue channel was surface treated to create an adhesive layer for attachment of extracellular matrix (collagen) hydrogel. First, poly D-lysine (1 mg/mL) was inserted into the main channel, and incubated at 37°C, 5% CO₂ for 45 minutes. The main channel was washed with deionized water, then 1% glutaraldehyde was inserted, and the device was incubated at room temperature for 1 hour 45 minutes. The devices were then thoroughly washed with deionized water and baked at 80°C overnight for dehydration.

Human umbilical vein ECs were seeded into the side channels (2×10^6 cells/mL in EC media) overnight. Human primary astrocytes (10×10^6 cells/mL) were embedded in collagen type I (rat tail) hydrogel (1 mg/mL) and injected into the central channel. Media were changed every 24 hours with combination of 50:50 astrocyte:EC media. Formation of EC monolayer and 3-dimensional astrocyte tissue was confirmed after 72 hours, then vehicle or medin (5 $\mu\text{mol/L}$) was infused (20 hours) on side channels of chips containing astrocytes and ECs, and chips with astrocytes but no ECs (schema

Table. Brain Donor Demographic Information

Variable	Cognitively Normal (N=21)	Vascular Dementia (N=25)	P Value
Age, y	81.4±2.4	88.9±1.5	0.01
Female sex, %	38	64	NS
Postmortem interval, h	3.2±0.2	3.1±0.1	NS
Mode of death, N (%)			
End-stage dementia	0 (0)	8 (38)	
Cardiovascular	6 (28)	6 (24)	
Malignancy	10 (48)	2 (8)	
Cerebrovascular accident	1 (5)	3 (12)	
Lung disease	1 (5)	5 (20)	
Renal disease	2 (10)	2 (8)	
Fracture/trauma	1 (5)	3 (12)	
Natural/not otherwise specified	0 (0)	3 (12)	

Data are given as mean±SEM, unless otherwise indicated.

summarized in Figure S2). Conditioned media interleukin-8 was measured using ELISA.

Statistical Analyses

Data are expressed as mean±SEM, and significant *P* value was set at *P*<0.05 (2 sided). Each data point represents a biologic replicate of independent experiments consistent with National Institutes of Health Rigor and Reproducibility Standards. Paired group analyses were done using paired *t* test (2 groups) or 1-way repeated-measures ANOVA (>2 groups) with pairwise post hoc analysis using Holm-Sidak. For data that do not have normal distribution or equal variance, natural log or square root transformation was performed, and analyses were done using normally distributed transformed data. If data remained non-normally distributed, Wilcoxon signed-rank test (2 groups) or 1-way repeated-measures ANOVA on ranks (>2 groups) with Dunn's post hoc pairwise testing was performed. Proportions were compared using Fisher's exact test. Unpaired groups were compared using unpaired *t* test. Analyses were done using Sigmasat 3.5 (Systat, San Jose, CA).

Results

Human Cerebral Collateral Arterial and Parenchymal Arteriole Medin Levels Are Higher in VaD Versus CN Donors

Overall, there were 21 clinicohistopathologically confirmed CN donors and 25 VaD donors (Table). VaD donors were

significantly older than CN donors. There were 64% female VaD donors and 38% female CN donors (*P*=not significant). To assess relevance of medin in CVD, we collected cerebral collateral arteries from VaD (N=11) and CN (N=12) brain donors and quantified arterial medin content. Overall cerebral collateral arterial medin was 5.9±1.2 ng medin/μg arterial protein (32±10 μmol/L). Arterial medin was higher in VaD compared with CN donors (Figure 1A). CWML score was higher in VaD versus CN donors (Figure 1B). Donors with higher CWML scores (median value or greater) had increased arterial medin compared with donors with lower scores (Figure 1C). In a separate set of donors, parenchymal cerebral arteriole medin was noted to be also higher in VaD compared with CN donors (Figure 1D and 1E). To assess degree of neuroinflammation, GFAP-expressing astrocytes, a marker of astrocyte activation,³⁷ were measured in the middle frontal gyrus. Activated astrocytes were higher in VaD versus CN brains (Figure 1D and 1F). In addition, astrocytes aggregated around cerebral arterioles (Figure 1D), with 73.5±5% of astrocytes within 100 μm of a cerebral arteriole versus 26.5±5% >100 μm (*P*=0.007).

Medin Induces EC Immune Activation and Cytotoxicity

We assessed immune activation and viability in ECs after 20-hour medin treatment. The dose selected (5 μmol/L) is within physiologic range of concentration found in human cerebral arteries on the basis of our results (32±10 μmol/L). Exposure to medin induced increased EC gene and protein expressions of interleukin-8, interleukin-6, ICAM-1, and PAI-1 (Figure 2A through 2H), with log-fold increases in interleukin-8, interleukin-6, and ICAM-1. Medin also caused reduced EC viability on the basis of reduced calcein-acetoxymethyl and increased annexin-V and propidium iodide fluorescence (Figure 2I through 2L). Medin caused immune activation response in human brain microvascular ECs similar to responses seen in human umbilical vein ECs, with increased gene expression of interleukin-8 (control versus medin-treated, relative to control: 1±0.2 versus 5.2±1.6; *P*=0.007; N=5), interleukin-6 (1±0.2 versus 5.8±1.7; *P*=0.005; N=5), and ICAM-1 (1±0.5 versus 9.5±0.1; *P*<0.001; N=3).

Expanding on our previous work,⁶ we now show that medin induces NFκB activation in ECs starting at 15 minutes, peaks at 1 hour, and persists for 20 hours after exposure (Figure S3A). Cotreatment with RO106-9920, a specific small-molecule inhibitor of NFκB-dependent cytokine expression,³⁰ abolished medin-induced increased gene expression of interleukin-8, interleukin-6, ICAM-1, and PAI-1 (Figure S3B through S3E), confirming that immune activation is NFκB dependent. Interestingly, cotreatment of medin with NFκB inhibitor did not improve EC viability (Figure S3F through S3H), suggesting that cytotoxicity is not NFκB dependent.

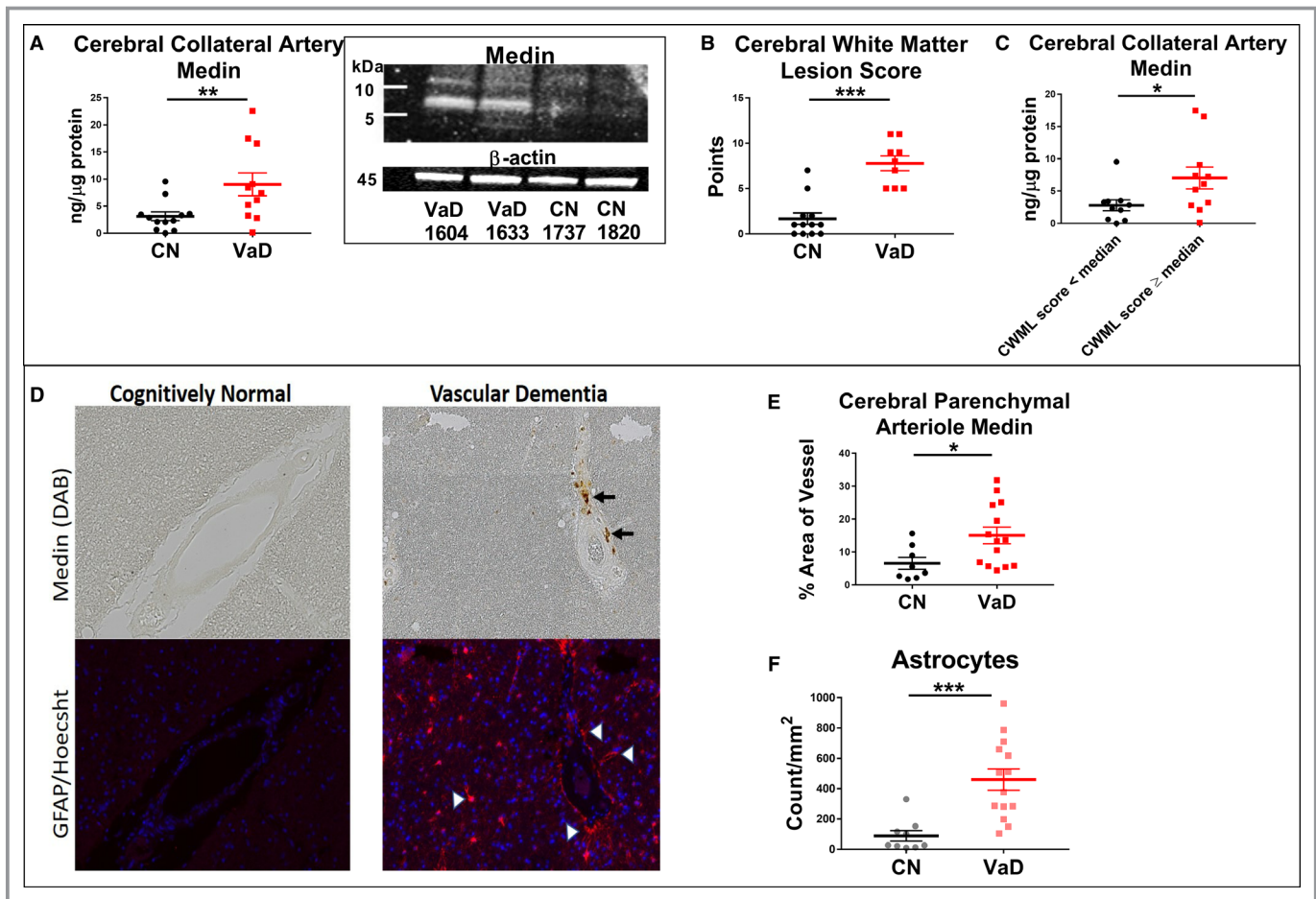


Figure 1. Cerebrovascular medin and astrocyte activation. **A**, Cerebral collateral artery medin was higher in vascular dementia (VaD) vs cognitively normal (CN). Insert shows Western blot of arterial medin (in monomer and dimer forms). **B** and **C**, Cerebral white matter lesion (CWML) scores from same donors were higher in VaD vs brain donors. Arterial medin was higher in donors with CWML scores equal to or greater than median value compared with those with lower scores. **D** through **F**, In a separate group of donors, middle frontal gyrus parenchymal cerebral arteriole medin (top figures in **D** shown in arrows) was higher in VaD vs CN (**E**). Activated astrocytes (anti-GFAP [glial fibrillary acidic protein] fluorescence, bottom figures in **D**, red pseudocolor and arrowheads) were higher in VaD vs CN donors (**F**), with abundance of astrocytes in close proximity to cerebral arteriole. Blue pseudocolor fluorescence signal is nuclear staining. Unpaired *t* test was used. DAB indicates 3,3'-diaminobenzidine. * $P < 0.05$, ** $P < 0.01$, *** $P < 0.001$.

NLGM1 Protects Against Immune Activation and Cytotoxicity of Medin

NLGM1 cotreatment with medin resulted in abolition of medin-induced increases in EC interleukin-8, interleukin-6, ICAM-1, and PAI-1 production (Figure 3A through 3H). It also prevented NF κ B activation by medin (Figure 3I). Unlike the findings with cotreatment with specific NF κ B inhibitor, NLGM1 cotreatment prevented medin cytotoxicity (Figure 3J through 3L).

To evaluate potential mechanism behind NLGM1 protection against medin, we assessed EC oxidative stress by measuring production of superoxide by flow cytometry (dihydroethidium fluorescence). Medin increased EC superoxide that was reversed by cotreatment with NLGM1 (Figure 4A). This protective effect was abolished when cotreated with brusatol, a

specific inhibitor of Nrf2.³⁸ Nrf2 controls the expression of an array of antioxidant response element-dependent genes and regulates antioxidant defense,³⁹ including expression of HO-1, NQO1, and SOD1. ECs treated with NLGM1 showed increased gene expression of HO-1 (control versus NLGM1, relative to control: 1 ± 0.04 versus 301.3 ± 83 ; $P < 0.001$; $N = 7$), NQO1 (1 ± 0.04 versus 16.3 ± 3.7 ; $P = 0.02$; $N = 7$), and SOD1 (1 ± 0.7 versus 1.9 ± 0.3 ; $P = 0.01$; $N = 8$). ECs treated with NLGM1 showed increase in nuclear Nrf2, and cotreatment of medin with NLGM1 increased nuclear Nrf2, HO-1, and NQO1 protein expression compared with medin treatment alone (Figure 4B through 4D). Addition of brusatol abolished the increase in HO-1 and NQO1 (Figure 4B through 4D).

To assess whether NLGM1 cytoprotection against medin is Nrf2 dependent, ECs were treated with medin alone and medin plus NLGM1, without or with brusatol. Results show

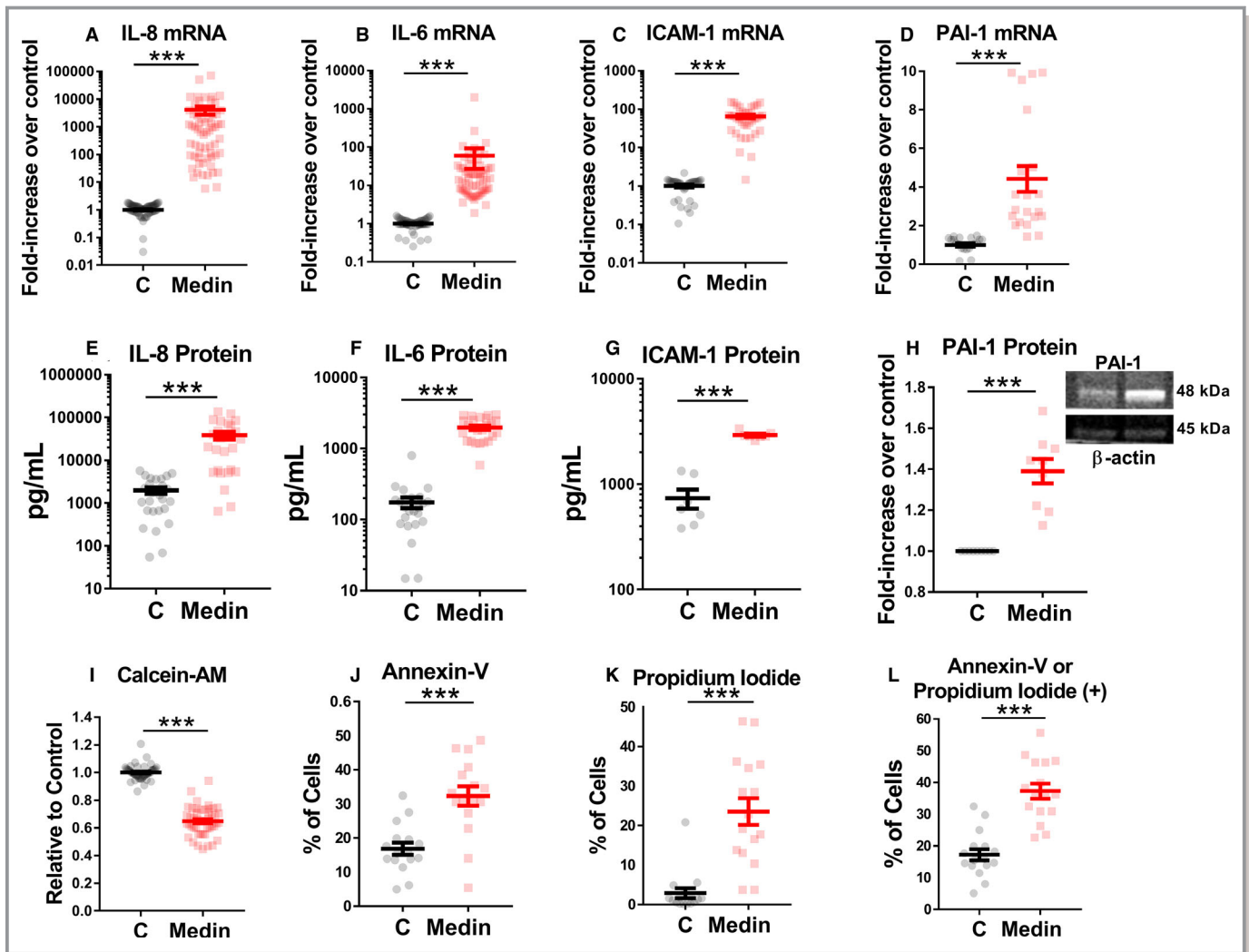


Figure 2. Medin causes endothelial cell (EC) immune activation and reduced viability. **A** through **H**, Medin caused increased gene (**A** through **D**) and protein (**E** through **H**) expressions of interleukin (IL)-8, IL-6, intercellular adhesion molecule-1 (ICAM-1), and plasminogen activator inhibitor-1 (PAI-1). **I** through **L**, Medin also caused reduced EC viability with reduced calcein-acetoxymethyl (AM) and increased annexin-V and propidium iodide fluorescence. Paired *t* test was used. C indicates control. ****P*<0.001.

that the protective effect of NLGM1 in terms of cell viability is reversed by brusatol (Figure 4E through 4G, Figure S4). To assess whether NLGM1 attenuation of medin-induced immune activation is Nrf-2 dependent, same treatments were performed, and immune activation markers were measured. Unlike viability assays, cotreatment with brusatol did not reverse NLGM1 protective effect against medin-induced increases in interleukin-8, interleukin-6, ICAM-1, and PAI-1 (Figure 4H through 4K).

ECs Modulate Astrocyte Activation After Medin Treatment

To evaluate the potential for medin-induced immune activation of ECs to affect astrocyte inflammatory response, monocultures of human astrocytes were exposed to vehicle control,

medin (5 μmol/L), conditioned media from ECs treated with vehicle, or conditioned media from ECs treated with medin (5 μmol/L) (Figure 5A). Results showed significant increase in astrocyte interleukin-8 production only when astrocytes were exposed to medin-treated EC media. After this, we developed a custom-built 3-dimensional cell coculture chip (Figure 5B), where the outer channels are infusible and seeded with ECs and the inner channel is seeded with collagen-encapsulated astrocytes with 100-μm gaps, allowing diffusion of agents from the outer EC layer to the inner astrocyte layer. Figure 5C shows the computer simulation with COMSOL Multiphysics software of 5 μmol/L medin administered through the side channels in media at 37°C and diffusing through the collagen hydrogel within the inner chamber. This demonstrates the extent of diffusion through the hydrogel at 5 minutes, and at 20 hours after administration, there is complete diffusion through the

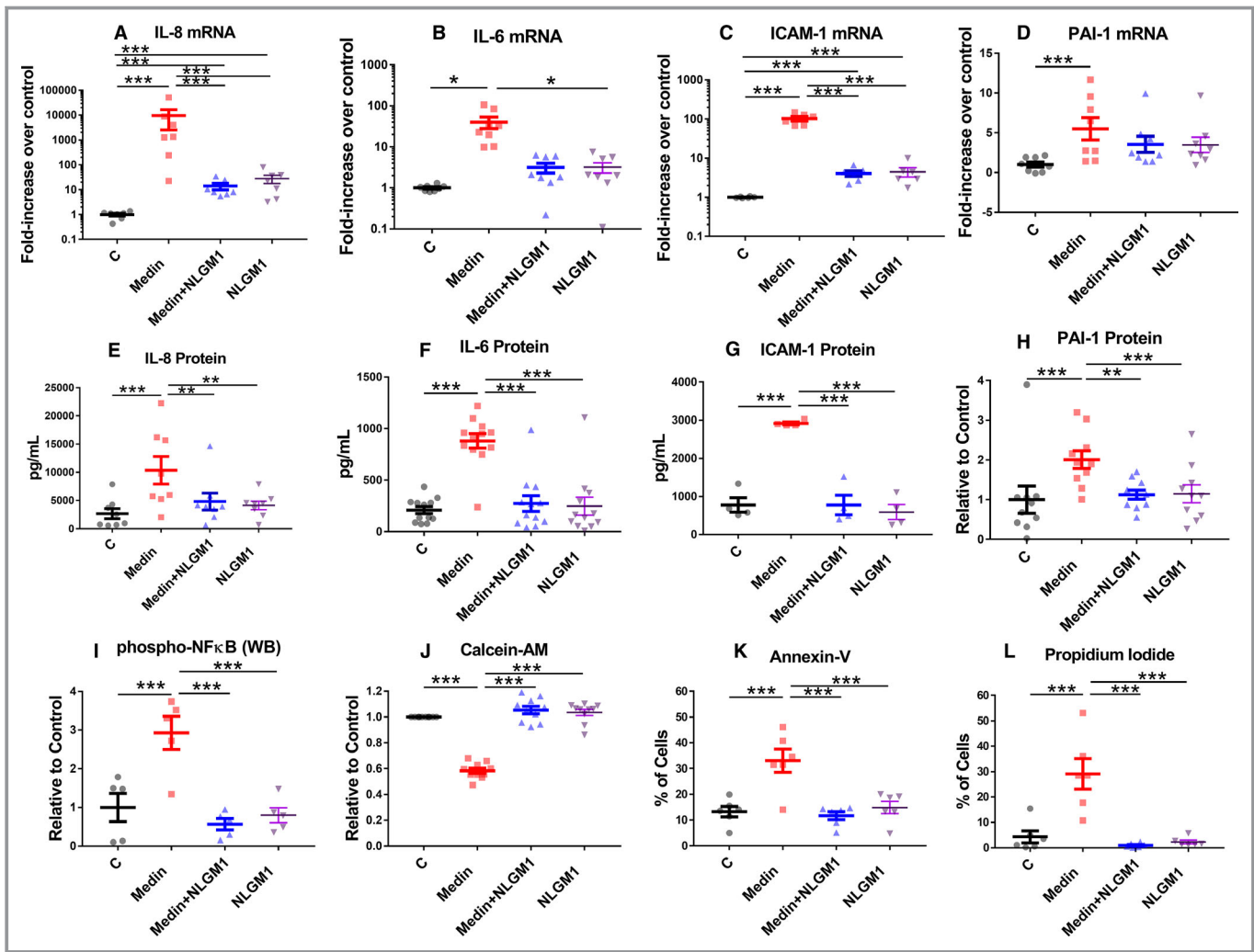


Figure 3. Monosialoganglioside-containing nanoliposomes (NLGM1) protect against medin-induced endothelial cell (EC) immune activation and reduced viability. Cotreatment of NLGM1 with medin reversed medin-induced increases in gene (A through D) and protein (E through H) expressions of interleukin (IL)-8, IL-6, intercellular adhesion molecule-1 (ICAM-1), and plasminogen activator inhibitor-1 (PAI-1), as well as nuclear factor- κ B (NF κ B) activation (I). Similarly, NLGM1 cotreatment restored EC viability in medin-treated cells (J through L). One-way repeated measures of ANOVA for all, except repeated-measures analysis on ranks for B. AM indicates acetoxymethyl; phospho-NF κ B, phosphorylated NF κ B; WB, Western blot. * P <0.05, ** P <0.01, *** P <0.001.

hydrogel, resulting in uniform concentration throughout, as predicted computationally. Experimentally, after seeding of the chip, astrocyte processes were seen to extend toward other astrocytes as well toward ECs (Figure 5D). Vehicle or medin was infused for 20 hours in outer channels in chips with or without seeded ECs. Astrocyte media interleukin-8 was shown to be higher in medin-treated chips with ECs when compared with medin-treated chips without ECs, showing modulation of astrocyte response by ECs exposed to medin (Figure 5E).

Discussion

The study presents the following novel findings. First, cerebral arteries from elderly human brain donors contain medin, and

arterial medin is higher in VaD compared with CN participants. Cerebral arterial medin was also higher in donors with higher cerebral white matter lesion scores. Second, medin induced human EC cytotoxicity and NF κ B-mediated immune activation with increased proinflammatory and prothrombotic cytokines (interleukin-8, interleukin-6, ICAM-1, and PAI-1). Third, we show that inflammatory astrocyte response was enhanced when exposed to medin-treated ECs or their conditioned media. Collectively, these findings suggest that medin could be a novel risk factor and treatment target for cerebrovascular inflammation that could modulate neuroinflammation. Last, we demonstrate that NLGM1, by inhibiting NF κ B activation and promoting Nrf2-dependent antioxidant responses, is a promising agent to reverse medin's adverse effects.

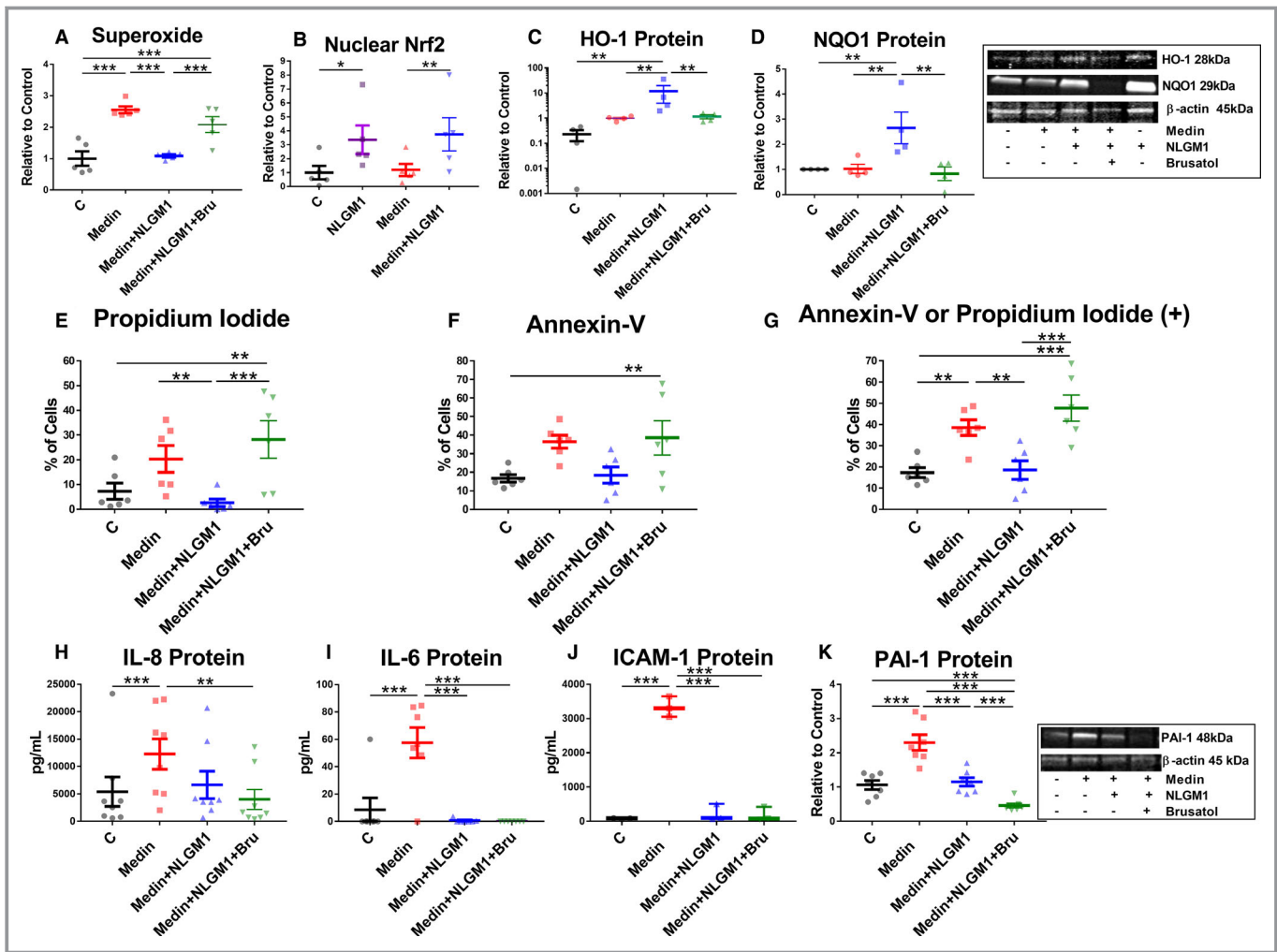


Figure 4. Monosialoganglioside-containing nanoliposomes (NLGM1) protection against medin cytotoxicity is nuclear factor erythroid 2-related factor 2 (Nrf2) dependent. **A**, Medin induces oxidative stress (increased superoxide) in endothelial cells (ECs) treated for 20 hours, which is reversed by NLGM1. The protective effect of NLGM1 is abolished by cotreatment of specific Nrf2 inhibitor brusato (Bru). **B**, ECs treated with NLGM1 show increased levels of nuclear Nrf2, whereas cotreatment with NLGM1 and medin resulted in increased nuclear Nrf2 compared with medin treatment alone. **C** and **D**, NLGM1 cotreatment with medin increased EC protein expression of heme oxygenase-1 (HO-1) and NAD(P)H quinone dehydrogenase-1 (NQO1), but this effect was abolished in the presence Bru. Representative Western blot images are shown to the right of the graph. **E** through **G**, NLGM1 cotreatment restored viability in ECs treated with medin, but this protection was abolished in the presence of Bru. **H** through **K**, Unlike effects on cellular viability, Bru cotreatment did not abolish the protective effect of NLGM1 against medin-induced EC immune activation. One-way repeated-measures ANOVA was used. ICAM-1 indicates intercellular adhesion molecule-1; IL, interleukin; PAI-1, plasminogen activator inhibitor-1. * $P < 0.05$, ** $P < 0.01$, *** $P < 0.001$.

Despite being one of the most common human amyloid proteins,^{4,5} little is known about the physiologic/pathologic effects of medin. On the basis of limited available data, medin has been proposed as a potential biologic agent influencing vascular aging⁴⁰ because of its aging-related deposition in blood vessels,^{6,7} the association between medin and aortic wall degeneration,⁸ and possible link with arterial inflammation.⁹ Aortic medin deposition is well documented, but there are lack of data, until now, on the prevalence of medin accumulation in cerebral vessels and its potential pathophysiologic role in CVD. Herein, we showed that medin is commonly found in cerebral collateral artery and parenchymal

arterioles of elderly individuals, with higher levels seen in VaD compared with CN donors. A potential pathologic contribution or association is supported by our observation that cerebral arterial medin is increased in donors with higher CWML scores. CWMLs are commonly seen in VaD and aging brains and are believed to be caused by ischemic microvascular injury; and their presence is associated with triple the risk of stroke and double the risk of dementia.^{14,24} Leptomeningeal arteries penetrate the cortex often, without branching to supply the subcortical white matter.⁴¹ White matter lesions have been shown to be strongly associated with leptomeningeal and parenchymal arteriole disease, and one

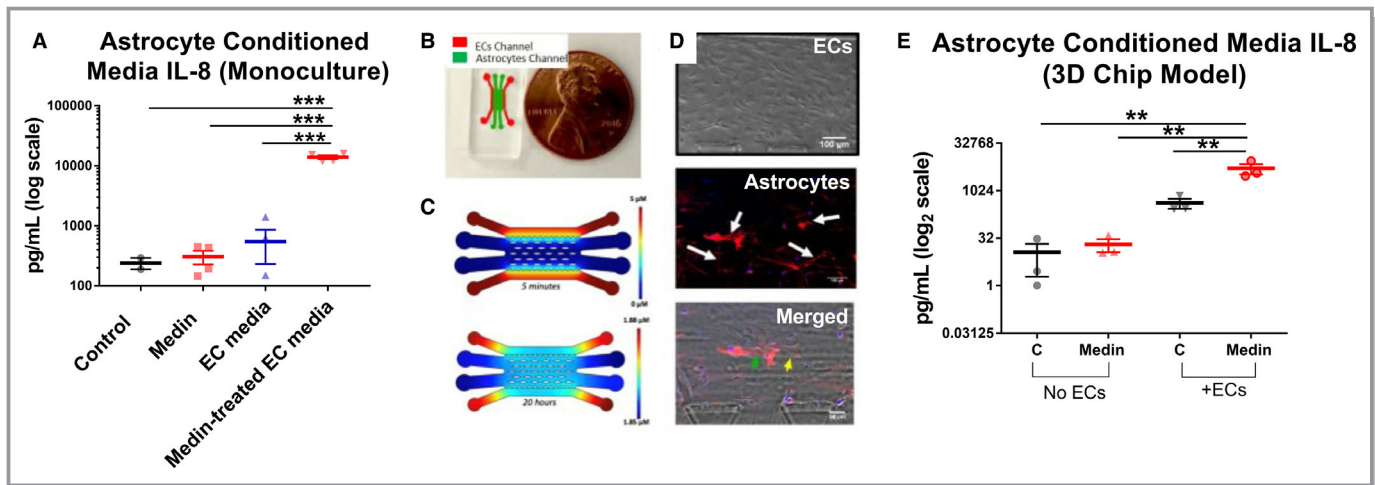


Figure 5. Medin-induced endothelial cell (EC) immune activation modulates astrocyte response. **A**, In astrocyte monocultures, interleukin (IL)-8 production was significantly higher when astrocytes were exposed to conditioned media of medin-treated ECs vs conditioned media of vehicle-treated ECs or direct exposure to medin. **B**, Three-dimensional (3D) chip with coculture of ECs (outer red channel) and astrocytes (central green channel). **C**, Computer simulation of medin diffusion through the chip shows complete medin diffusion and expected uniform concentration after 20 hours. **D**, Astrocyte processes are seen extending toward other astrocytes (white arrows) as well as toward ECs (green and yellow arrows). **E**, Astrocyte chamber conditioned media show higher IL-8 production in the presence of medin-treated ECs vs vehicle-treated ECs or in the absence of ECs with astrocytes exposed to either medin or vehicle. One-way ANOVA was used. C indicates control. *** $P < 0.001$, ** $P < 0.01$.

mechanism proposed involved obstruction of drainage, leading to dilated perivascular spaces around arteries in the white matter.^{41,42} The pathologic role of medin is further supported mechanically by our previous findings that medin causes endothelial dysfunction in human cerebral arterioles⁶ and our current findings showing a more extensive immune activation effect of medin on ECs with increased ICAM-1, PAI-1, interleukin-8, and interleukin-6. ICAM-1 is a transmembrane protein that facilitates leukocyte adhesion and endothelial transmigration⁴³; it also has proinflammatory signal transduction effects that promote leukocyte and macrophage recruitment.⁴⁴ ICAM-1 is elevated in subarachnoid hemorrhage⁴⁵ and ischemic stroke,⁴⁶ biologic nidus for later development of VaD.⁴⁷ PAI-1 inhibits tissue plasminogen activator and urokinase, which are plasminogen activators; by doing so, PAI-1 inhibits plasmin-mediated fibrinolysis and is prothrombotic.⁴⁸ Consistent with our results, PAI-1 expression was shown by others to be increased by NF κ B-mediated inflammatory stimuli.⁴⁹ Elevated PAI-1 was reported in VaD patients, and hemostasis abnormalities were more frequent and marked in VaD compared with Alzheimer disease.⁵⁰ Interleukin-8 and interleukin-6 function as leukocyte chemoattractants.⁵¹ Plasma interleukin-6 was noted to be independently associated with functional impairment in older individuals with VaD but not Alzheimer disease.⁵² Levels of interleukin-8 correlated with severity of cognitive impairment in VaD.⁵³ Our finding that medin causes EC immune activation when placed in the context of our observation that cerebral arteriole medin is increased in VaD and in donors with higher

CWML scores suggests a potential role for medin in VaD pathophysiological characteristics.

Established mechanisms linking small-vessel CVD and VaD include hypoxic/ischemic injury from vessel occlusion/flow-limiting obstruction, vascular microbleeds, and lipohyalinosis; the latter involves the interplay of vascular inflammation and reactive gliosis of astrocytes, microglia, and oligodendrocytes, leading to connective tissue hyaline deposition that disrupts blood-brain barrier integrity.⁵⁴ Histopathologic analysis showed that CWMLs were associated with both endothelial and glial activation.¹³ Our findings showed increased GFAP-expressing astrocytes in VaD brains with an interesting observation that more astrocytes are closer (within 100 μ m) to a cerebral arteriole than farther away. Our astrocyte monoculture and chip EC-astrocyte coculture data show that interleukin-8 production is enhanced when astrocytes are exposed to medin-treated ECs. Although our in vitro models did not specifically explore which EC product induced astrocyte activation, as manifested by increased interleukin-8 production, it is well known that astrocytes are effector targets of cytokines and chemokines having multiple receptors for inflammatory mediators that could initiate activation.⁵⁵ These in vitro and brain histology results support a possible modulating role of medin-induced EC immune activation in enhancing neuroinflammation. Neuroinflammatory mechanisms are suspected to play an important role in VaD.^{53,56} Because inflammatory cytokine-mediated interactions between glia cells and neurons could contribute to cognitive impairment,^{12,15,57} it is reasonable to speculate that

medin might also modulate cognitive function through vascular inflammatory mechanisms.

Medin-mediated EC immune activation is dependent on NFκB activation, a critical primary transcription factor regulating cellular immune response,⁵⁸ as shown by the reversal by RO106-9920, a selective inhibitor of IκBα degradation and NFκB activation.³⁰ NLGM1 also inhibited NFκB activation, leading to reversal of medin-induced increases in interleukin-8, interleukin-6, ICAM-1, and PAI-1. However, NFκB inhibition by RO1-169920 did not restore EC viability after exposure to medin, suggesting distinct signaling mechanisms between immune activation and cellular viability. NLGM1, unlike RO1-169920, fully restored EC viability. One of the potential mechanisms by which medin activates NFκB is through receptor for advanced glycation end product signaling, as we have previously shown that medin cotreated with specific receptor for advanced glycation end product inhibitor FPS-ZM1 prevented medin-induced NFκB activation.⁶ In addition, reactive oxygen species can activate NFκB, which is known to be a reduction-oxidation sensitive factor.⁵⁹ Our data showing medin causing EC oxidative stress and NLGM1 preventing medin-induced EC immune activation through Nrf2-dependent mechanism support this potential additional mechanism.

We previously showed that NLGM1 induced activation of Nrf2 (manifested by nuclear translocation from cytosol), a transcription factor that regulates expression of antioxidant proteins to protect against oxidative damage,³⁹ leading to protection of ECs against light chain amyloid injury.¹⁹ Similar to effects observed with light chain amyloid protein, medin increased EC superoxide. Despite inducing oxidative stress, no accompanying Nrf2 activation was elicited by medin, nor change in antioxidant HO-1 and NQO1 expression. NLGM1 cotreatment led to reduced EC superoxide; it increased nuclear Nrf2 and gene expression of HO-1, NQO1, and SOD1, 3 Nrf2-dependent antioxidant enzymes.^{60–62} SOD1 is a cytosolic superoxide dismutase that catalyze the dismutation of superoxide anion. We previously showed that a form of superoxide dismutase, polyethylene glycol SOD, prevented medin-induced human microvascular endothelial dysfunction and reduced EC superoxide levels.⁶ The cytoprotective effect of NLGM1 against medin is confirmed to be Nrf2 dependent because cotreatment with brusatol, a specific inhibitor of Nrf2,³⁸ reversed the protective effect of NLGM1 on superoxide production and EC cell viability while preventing increases in antioxidant enzymes HO-1 and HOO1. Interestingly, Nrf2 inhibition did not prevent NLGM1 from reversing medin-induced EC immune activation, again suggesting distinct signaling mechanisms. Our findings that NLGM1 restored EC viability and prevented immune activation by medin point to a promising novel agent and therapeutic approach

against medin-induced vasculopathy. We previously showed that NLGM1 can also protect against amyloid light chain-induced oxidative stress by the same mechanism.³⁹ Structural and pathological^{63,64} similarities between amyloid proteins are well established. Accordingly, NLGM1 might also be protective in other amyloid conditions, representing an exciting new therapeutic avenue.

Limitations

This initial investigation has important limitations that must be addressed in future studies. In vitro experiments involve short-term experiments (20 hours), and longer-term exposure effects, including in vivo preclinical studies, must be pursued. Future effort should also be focused on identifying the cleavage enzyme/s responsible for endogenous medin production that could be manipulated to probe effects of endogenous medin production. The study was limited to studying medin's effect on astrocyte activation, but future models should include other glial components (microglia and oligodendrocytes) as well as neurons to fully explore medin's effects on vasculoneural inflammatory coupling, while also systematically investigating full effects on astrocyte function. Although our study showed immune activation of ECs by medin, the functional significance of increased proinflammatory cytokine production needs to be empirically determined in future in vivo studies or triculture 3-dimensional models that include ECs, glial cells, and neurons. The sample size of brain tissues analyzed should be expanded to fully establish association between cerebrovascular medin and neuropathologic

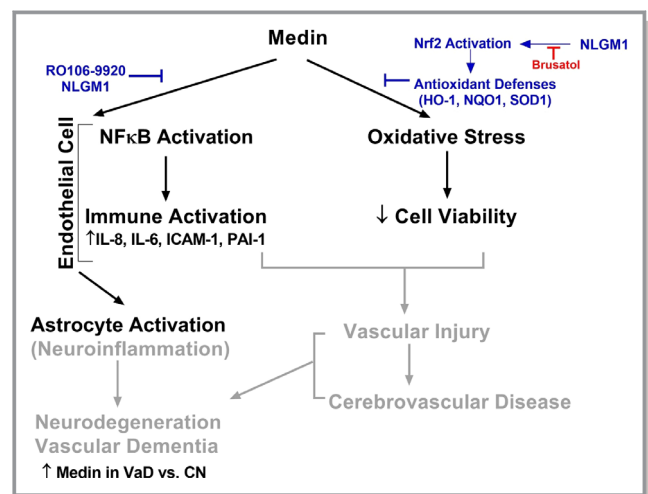


Figure 6. Proposed schema of medin's biologic effects. CN indicates cognitively normal; HO-1, heme oxygenase-1; ICAM-1, intercellular adhesion molecule-1; IL, interleukin; NFκB, nuclear factor-κB; NLGM1, monosialoganglioside-containing nanoliposomes; NQO1, NAD(P)H quinone dehydrogenase-1; Nrf2, nuclear factor erythroid 2-related factor 2; PAI-1, plasminogen activator inhibitor-1; SOD1, superoxide dismutase 1; VaD, vascular dementia.

outcomes (neuroinflammation, neurodegeneration, and cognitive dysfunction), with inclusion of nonelderly brain tissues wherever available.

Conclusions

The biologic effects of medin, one of the most common human amyloid proteins, are unknown. We showed, for the first time, the prevalence of medin in cerebral arteries of elderly brain donors, with higher values in VaD compared with CN patients and increased arterial medin in donors with higher CWML scores. Medin impaired EC viability and induced profound endothelial immune activation that modulated astrocyte activation. The findings point to the potential role of medin in vascular inflammation, which, in turn, could modulate neuroinflammation, making it a promising candidate target to elucidate the pathophysiological characteristics of aging-related CVD and VaD (proposed schema in Figure 6). NLGM1, via effects on NF κ B and Nrf2 signaling, reverses medin's adverse effects and represents a potential novel therapeutic approach.

Acknowledgments

We thank our research volunteers, John Hatfield, Gail Farrell, Carl T. Hayden Medical Research Foundation, and Phoenix Veterans Affairs Office of Research.

Sources of Funding

This work was supported by US Department of Veterans Affairs (Merit BX007080), Department of Defense (W81XWH-17-1-0473), National Institutes of Health (NINDSU24NS072026/NIAP30AG19610/NIARO1 AG019795), British Heart Foundation (FS/12/61/29877), Arizona Department of Health Services (211002), Arizona Biomedical Research Commission (4001/0011/05-901/10010), and Michael J. Fox Foundation. The study was based on work supported by the Department of Veterans Affairs and Department of Veterans Affairs Employment. The contents of the work do not represent the views of the Department of Veterans Affairs or the US government.

Disclosures

A patent application has been filed for use of nanoliposomes for medin vasculopathy. The authors named for the patent application are: Karamanova, Truran, Weissig, Madine, Davies, and Migrino.

References

1. Yoshitake T, Kiyohara Y, Kato I, Ohmura T, Iwamoto H, Nakayama K, Ohmori S, Nomiyama K, Kawano H, Ueda K, Sueshi K, Tsuneyoshi M, Fujishima M.

Incidence and risk factors of vascular dementia and Alzheimer's disease in a defined elderly Japanese population: the Hisayama Study. *Neurology*. 1995;45:1161–1168.

2. Ungvari Z, Buffenstein R, Austad SN, Podlutzky A, Kaley G, Csiszar A. Oxidative stress in vascular senescence: lessons from successfully aging species. *Front Biosci*. 2008;13:5056–5070.
3. Ungvari Z, Kaley G, de Cabo R, Sonntag WE, Csiszar A. Mechanisms of vascular aging: new perspectives. *J Gerontol A Biol Sci Med Sci*. 2010;65:1028–1041.
4. Haggqvist B, Naslund J, Sletten K, Westermark GT, Mucchiano G, Tjernberg LO, Nordstedt C, Engstrom U, Westermark P. Medin: an integral fragment of aortic smooth muscle cell-produced lactadherin forms the most common human amyloid. *Proc Natl Acad Sci USA*. 1999;96:8669–8674.
5. Larsson A, Soderberg L, Westermark GT, Sletten K, Engstrom U, Tjernberg LO, Naslund J, Westermark P. Unwinding fibril formation of medin, the peptide of the most common form of human amyloid. *Biochem Biophys Res Commun*. 2007;361:822–828.
6. Migrino RQ, Davies HA, Truran S, Karamanova N, Franco DA, Beach TG, Serrano GE, Truong D, Nikkiah M, Madine J. Amyloidogenic medin induces endothelial dysfunction and vascular inflammation through the receptor for advanced glycation endproducts. *Cardiovasc Res*. 2017;113:1389–1402.
7. Peng S, Glennert J, Westermark P. Medin-amyloid: a recently characterized age-associated arterial amyloid form affects mainly arteries in the upper part of the body. *Amyloid*. 2005;12:96–102.
8. Peng S, Larsson A, Wassberg E, Gerwins P, Thelin S, Fu X, Westermark P. Role of aggregated medin in the pathogenesis of thoracic aortic aneurysm and dissection. *Lab Invest*. 2007;87:1195–1205.
9. Peng S, Westermark GT, Naslund J, Haggqvist B, Glennert J, Westermark P. Medin and medin-amyloid in ageing inflamed and non-inflamed temporal arteries. *J Pathol*. 2002;196:91–96.
10. Migrino RQ, Truran S, Karamanova N, Serrano GE, Madrigal C, Davies HA, Madine J, Reaven P, Beach TG. Human cerebral collateral arteriole function in subjects with normal cognition, mild cognitive impairment, and dementia. *Am J Physiol Heart Circ Physiol*. 2018;315:H284–H290.
11. Simpson JE, Fernando MS, Clark L, Ince PG, Matthews F, Forster G, O'Brien JT, Barber R, Kalaria RN, Brayne C, Shaw PJ, Lewis CE, Wharton SB; MRC Cognitive Function and Ageing Neuropathology Study Group. White matter lesions in an unselected cohort of the elderly: astrocytic, microglial and oligodendrocyte precursor cell responses. *Neuropathol Appl Neurobiol*. 2007;33:410–419.
12. Rosenberg GA. Inflammation and white matter damage in vascular cognitive impairment. *Stroke*. 2009;40:S20–S23.
13. Fernando MS, O'Brien JT, Perry RH, English P, Forster G, McMeekin W, Slade JY, Golkhar A, Matthews FE, Barber R, Kalaria RN, Ince PG; Neuropathology Group of MRC CFAS. Comparison of the pathology of cerebral white matter with post-mortem magnetic resonance imaging (MRI) in the elderly brain. *Neuropathol Appl Neurobiol*. 2004;30:385–395.
14. Wardlaw JM, Valdes Hernandez MDC, Munoz Maniega S. What are white matter hyperintensities made of? Relevance to vascular cognitive impairment. *J Am Heart Assoc*. 2015;4:e001140. DOI: 10.1161/JAHA.114.001140.
15. Heppner FL, Ransohoff RM, Becher B. Immune attack: the role of inflammation in Alzheimer disease. *Nat Rev Neurosci*. 2015;16:358–372.
16. Equils O, Naiki Y, Shapiro AM, Michelsen K, Lu D, Adams J, Jordan S. 1,25-Dihydroxyvitamin D inhibits lipopolysaccharide-induced immune activation in human endothelial cells. *Clin Exp Immunol*. 2006;143:58–64.
17. Leung DY, Cotran RS, Kurt-Jones E, Burns JC, Newburger JW, Pober JS. Endothelial cell activation and high interleukin-1 secretion in the pathogenesis of acute Kawasaki disease. *Lancet*. 1989;2:1298–1302.
18. Opitz B, Forster S, Hocke AC, Maass M, Schmeck B, Hippenstiel S, Suttorp N, Krull M. Nod1-mediated endothelial cell activation by *Chlamydophila pneumoniae*. *Circ Res*. 2005;96:319–326.
19. Franco DA, Truran S, Weissig V, Guzman-Villanueva D, Karamanova N, Senapati S, Burciu C, Ramirez-Alvarado M, Blancas-Mejia LM, Lindsay S, Hari P, Migrino RQ. Monosialoganglioside-containing nanoliposomes restore endothelial function impaired by AL amyloidosis light chain proteins. *J Am Heart Assoc*. 2016;5:e003318. DOI: 10.1161/JAHA.116.003318.
20. Truran S, Weissig V, Madine J, Davies HA, Guzman-Villanueva D, Karamanova N, Serrano G, Beach TG, Migrino RQ. Nanoliposomes protect against human arteriole endothelial dysfunction induced by B-amyloid peptide. *J Cereb Blood Flow Metab*. 2015;36:405–412.
21. Beach TG, Adler CH, Sue LI, Serrano G, Shill HA, Walker DG, Lue L, Roher AE, Dugger BN, Maarouf C, Birdsill AC, Intorcchia A, Saxon-Labelle M, Pullen J, Scroggins A, Filon J, Scott S, Hoffman B, Garcia A, Caviness JN, Hentz JG, Driver-Dunckley E, Jacobson SA, Davis KJ, Belden CM, Long KE, Malek-Ahmadi

- M, Powell JJ, Gale LD, Nicholson LR, Caselli RJ, Woodruff BK, Rapsack SZ, Ahern GL, Shi J, Burke AD, Reiman EM, Sabbagh MN. Arizona Study of Aging and Neurodegenerative Disorders and brain and body donation program. *Neuropathology*. 2015;35:354–389.
22. Roman GC, Tatemichi TK, Erkinjuntti T, Cummings JL, Masdeu JC, Garcia JH, Amaducci L, Orgogozo JM, Brun A, Hofman A, et al. Vascular dementia: diagnostic criteria for research studies: report of the NINDS-AIREN International Workshop. *Neurology*. 1993;43:250–260.
 23. Davies HA, Wilkinson MC, Gibson RP, Middleton DA. Expression and purification of the aortic amyloid polypeptide medin. *Protein Expr Purif*. 2014;98:32–37.
 24. Prins ND, Scheltens P. White matter hyperintensities, cognitive impairment and dementia: an update. *Nat Rev Neurol*. 2015;11:157–165.
 25. Choi SA, Evidente VG, Caviness JN, Shill HA, Sabbagh MN, Connor DJ, Hentz JG, Adler CH, Beach TG. Are there differences in cerebral white matter lesion burdens between Parkinson's disease patients with or without dementia? *Acta Neuropathol*. 2010;119:147–149.
 26. Kitazume S, Tachida Y, Kato M, Yamaguchi Y, Honda T, Hashimoto Y, Wada Y, Saito T, Iwata N, Saido T, Taniguchi N. Brain endothelial cells produce amyloid beta from amyloid precursor protein 770 and preferentially secrete the O-glycosylated form. *J Biol Chem*. 2010;285:40097–40103.
 27. Ma JF, Wang HM, Li QY, Zhang Y, Pan J, Qiang Q, Xin XY, Tang HD, Ding JQ, Chen SD. Starvation triggers Abeta42 generation from human umbilical vascular endothelial cells. *FEBS Lett*. 2010;584:3101–3106.
 28. Chao AC, Lee TC, Juo SH, Yang DI. Hyperglycemia increases the production of amyloid beta-peptide leading to decreased endothelial tight junction. *CNS Neurosci Ther*. 2016;22:291–297.
 29. Gomez-Gavro MV, Scott CE, Sesay AK, Matheu A, Booth S, Galichet C, Lovell-Badge R. Betacellulin promotes cell proliferation in the neural stem cell niche and stimulates neurogenesis. *Proc Natl Acad Sci USA*. 2012;109:1317–1322.
 30. Swinney DC, Xu YZ, Scarafia LE, Lee I, Mak AY, Gan QF, Ramesha CS, Mulkins MA, Dunn J, So OY, Biegel T, Dinh M, Volkel P, Barnett J, Dalrymple SA, Lee S, Huber M. A small molecule ubiquitination inhibitor blocks NF-kappa B-dependent cytokine expression in cells and rats. *J Biol Chem*. 2002;277:23573–23581.
 31. Bindokas VP, Jordan J, Lee CC, Miller RJ. Superoxide production in rat hippocampal neurons: selective imaging with hydroethidine. *J Neurosci*. 1996;16:1324–1336.
 32. Neri S, Mariani E, Meneghetti A, Cattini L, Facchini A. Calcein-acetyoxymethyl cytotoxicity assay: standardization of a method allowing additional analyses on recovered effector cells and supernatants. *Clin Diagn Lab Immunol*. 2001;8:1131–1135.
 33. Migrino RQ, Truran S, Gutterman DD, Franco DA, Bright M, Schlundt B, Timmons M, Motta A, Phillips SA, Hari P. Human microvascular dysfunction and apoptotic injury induced by AL amyloidosis light chain proteins. *Am J Physiol Heart Circ Physiol*. 2011;301:H2305–H2312.
 34. Nagaraju S, Truong D, Mouneimne G, Nikkiah M. Microfluidic tumor-vascular model to study breast cancer cell invasion and intravasation. *Adv Healthc Mater*. 2018;7:e1701257.
 35. Truong D, Fiorelli R, Barrientos E, Melendez E, Sanai N, Mehta S, Nikkiah M. A three-dimensional (3D) organotypic microfluidic model for glioma stem cells-vascular interactions. *Biomaterials*. 2019;198:63–77.
 36. Truong DD, Kratz A, Park JG, Barrientos ES, Saini H, Nguyen T, Pockaj B, Mouneimne G, LaBaer J, Nikkiah M. A human organotypic microfluidic tumor model permits investigation of the interplay between patient-derived fibroblasts and breast cancer cells. *Cancer Res*. 2019;79:3139–3151.
 37. Brahmachari S, Fung YK, Pahan K. Induction of glial fibrillary acidic protein expression in astrocytes by nitric oxide. *J Neurosci*. 2006;26:4930–4939.
 38. Olayanju A, Copples IM, Bryan HK, Edge GT, Sison RL, Wong MW, Lai ZQ, Lin ZX, Dunn K, Sanderson CM, Alghanem AF, Cross MJ, Ellis EC, Ingelman-Sundberg M, Malik HZ, Kitteringham NR, Goldring CE, Park BK. Brusatol provokes a rapid and transient inhibition of Nrf2 signaling and sensitizes mammalian cells to chemical toxicity-implications for therapeutic targeting of Nrf2. *Free Radic Biol Med*. 2015;78:202–212.
 39. Ma Q. Role of nrf2 in oxidative stress and toxicity. *Annu Rev Pharmacol Toxicol*. 2013;53:401–426.
 40. Lakatta EG. The reality of aging viewed from the arterial wall. *Artery Res*. 2013;7:73–80.
 41. Weller RO, Hawkes CA, Kalaria RN, Werring DJ, Carare RO. White matter changes in dementia: role of impaired drainage of interstitial fluid. *Brain Pathol*. 2015;25:63–78.
 42. Roher AE, Kuo YM, Esh C, Knebel C, Weiss N, Kalback W, Luehrs DC, Childress JL, Beach TG, Weller RO, Kokjohn TA. Cortical and leptomeningeal cerebrovascular amyloid and white matter pathology in Alzheimer's disease. *Mol Med*. 2003;9:112–122.
 43. Yang L, Froio RM, Sciuto TE, Dvorak AM, Alon R, Luscinskas FW. ICAM-1 regulates neutrophil adhesion and transcellular migration of TNF-alpha-activated vascular endothelium under flow. *Blood*. 2005;106:584–592.
 44. Etienne-Manneville S, Chaverot N, Strosberg AD, Couraud PO. ICAM-1-coupled signaling pathways in astrocytes converge to cyclic AMP response element-binding protein phosphorylation and TNF-alpha secretion. *J Immunol*. 1999;163:668–674.
 45. Polin RS, Bavbek M, Shaffrey ME, Billups K, Bogaev CA, Kassell NF, Lee KS. Detection of soluble E-selectin, ICAM-1, VCAM-1, and L-selectin in the cerebrospinal fluid of patients after subarachnoid hemorrhage. *J Neurosurg*. 1998;89:559–567.
 46. Frijns CJ, Kappelle LJ. Inflammatory cell adhesion molecules in ischemic cerebrovascular disease. *Stroke*. 2002;33:2115–2122.
 47. Corraini P, Henderson VW, Ording AG, Pedersen L, Horvath-Puho E, Sorensen HT. Long-term risk of dementia among survivors of ischemic or hemorrhagic stroke. *Stroke*. 2017;48:180–186.
 48. Vaughan DE. PAI-1 and atherothrombosis. *J Thromb Haemost*. 2005;3:1879–1883.
 49. Kruithof EK. Regulation of plasminogen activator inhibitor type 1 gene expression by inflammatory mediators and statins. *Thromb Haemost*. 2008;100:969–975.
 50. Mari D, Parnetti L, Coppola R, Bottasso B, Reboldi GP, Senin U, Mannucci PM. Hemostasis abnormalities in patients with vascular dementia and Alzheimer's disease. *Thromb Haemost*. 1996;75:216–218.
 51. Mantovani A, Bussolino F, Dejana E. Cytokine regulation of endothelial cell function. *FASEB J*. 1992;6:2591–2599.
 52. Zuliani G, Guerra G, Ranzini M, Rossi L, Munari MR, Zurlo A, Ble A, Volpato S, Atti AR, Fellin R. High interleukin-6 plasma levels are associated with functional impairment in older patients with vascular dementia. *Int J Geriatr Psychiatry*. 2007;22:305–311.
 53. Schmitz M, Hermann P, Oikonomou P, Stoeck K, Ebert E, Poliakov T, Schmidt C, Llorens F, Zafar S, Zerr I. Cytokine profiles and the role of cellular prion protein in patients with vascular dementia and vascular encephalopathy. *Neurobiol Aging*. 2015;36:2591–2606.
 54. Shabir O, Berwick J, Francis SE. Neurovascular dysfunction in vascular dementia, Alzheimer's and atherosclerosis. *BMC Neurosci*. 2018;19:62.
 55. Sofroniew MV. Multiple roles for astrocytes as effectors of cytokines and inflammatory mediators. *Neuroscientist*. 2014;20:160–172.
 56. Iadecola C. The overlap between neurodegenerative and vascular factors in the pathogenesis of dementia. *Acta Neuropathol*. 2010;120:287–296.
 57. Rubio-Perez JM, Morillas-Ruiz JM. A review: inflammatory process in Alzheimer's disease, role of cytokines. *ScientificWorldJournal*. 2012;2012:756357.
 58. Gilmore TD. Introduction to NF-kappaB: players, pathways, perspectives. *Oncogene*. 2006;25:6680–6684.
 59. Kabe Y, Ando K, Hirao S, Yoshida M, Handa H. Redox regulation of NF-kappaB activation: distinct redox regulation between the cytoplasm and the nucleus. *Antioxid Redox Signal*. 2005;7:395–403.
 60. Araujo JA, Zhang M, Yin F. Heme oxygenase-1, oxidation, inflammation, and atherosclerosis. *Front Pharmacol*. 2012;3:119.
 61. Dinkova-Kostova AT, Talalay P. NAD(P)H:quinone acceptor oxidoreductase 1 (NQO1), a multifunctional antioxidant enzyme and exceptionally versatile cytoprotector. *Arch Biochem Biophys*. 2010;501:116–123.
 62. Yan D, Dong J, Sulik KK, Chen SY. Induction of the Nrf2-driven antioxidant response by tert-butylhydroquinone prevents ethanol-induced apoptosis in cranial neural crest cells. *Biochem Pharmacol*. 2010;80:144–149.
 63. Schubert D, Behl C, Lesley R, Brack A, Dargusch R, Sagara Y, Kimura H. Amyloid peptides are toxic via a common oxidative mechanism. *Proc Natl Acad Sci USA*. 1995;92:1989–1993.
 64. Pastor MT, Kummerer N, Schubert V, Esteras-Chopo A, Dotti CG, Lopez de la Paz M, Serrano L. Amyloid toxicity is independent of polypeptide sequence, length and chirality. *J Mol Biol*. 2008;375:695–707.

SUPPLEMENTAL MATERIAL

Figure S1. 2D astrocyte culture treatment scheme. Experimental design involved with exposure of astrocyte 2D culture to vehicle, medin, media from HUVECs treated with vehicle or medin. The EC conditioned media IL-8 contents were 2626 ± 766 pg/ml (range 329-3391 pg/ml) for vehicle-treated ECs and 19441 ± 6950 pg/ml (range 12492-40290 pg/ml) for medin-treated ECs. EC-endothelial cell, ELISA-enzyme linked immunosorbent assay, CM-conditioned media

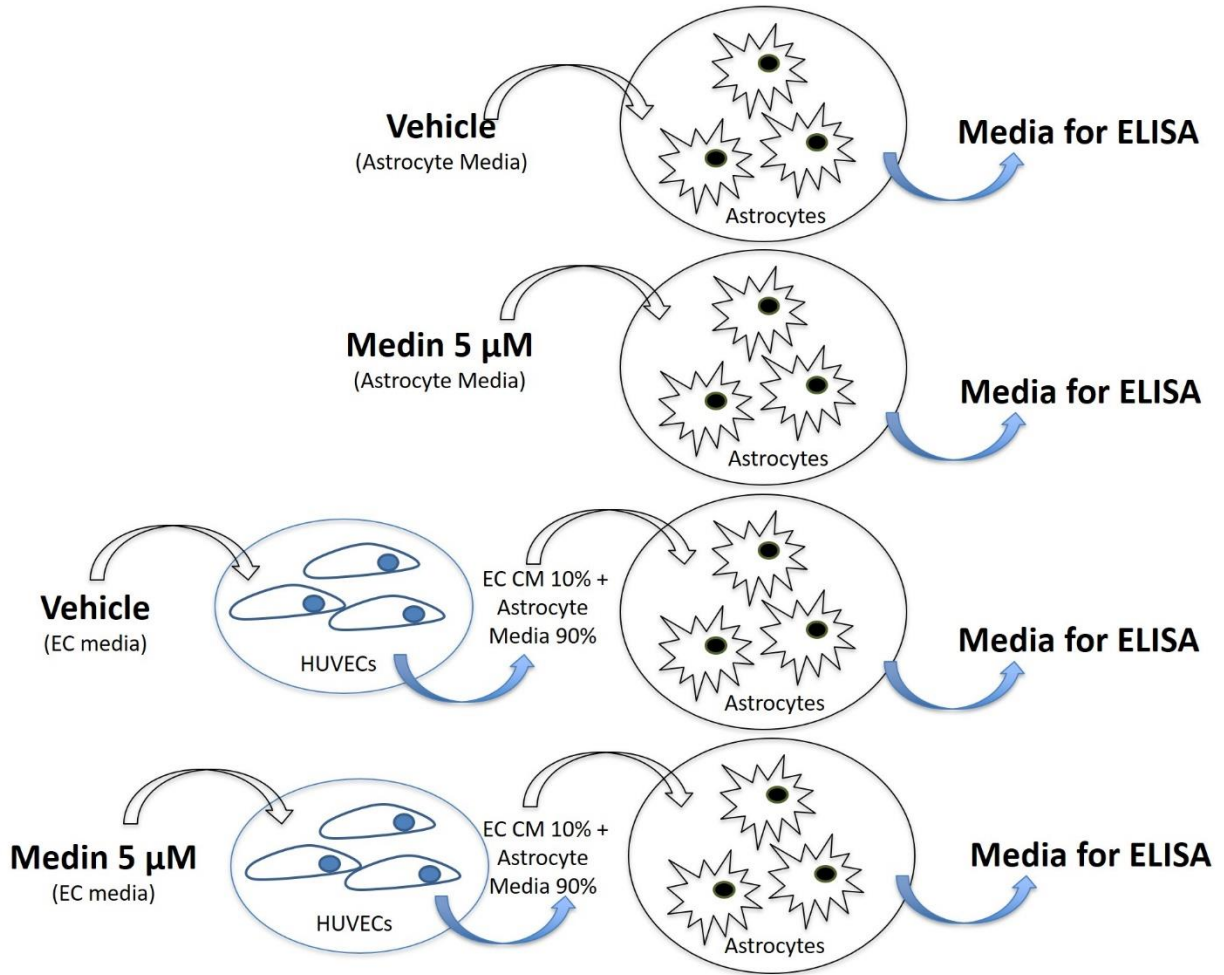


Figure S2. 3D chip model treatment scheme. Astrocytes were seeded in central chambers of microfluidic chip, while side chambers either had no or seeded ECs. Vehicle or medin (5 μ M) was infused on side channels and cells exposed to treatment for 20 hours. Conditioned media were collected for IL-8 measurement by ELISA. ELISA=enzyme linked immunosorbent assay

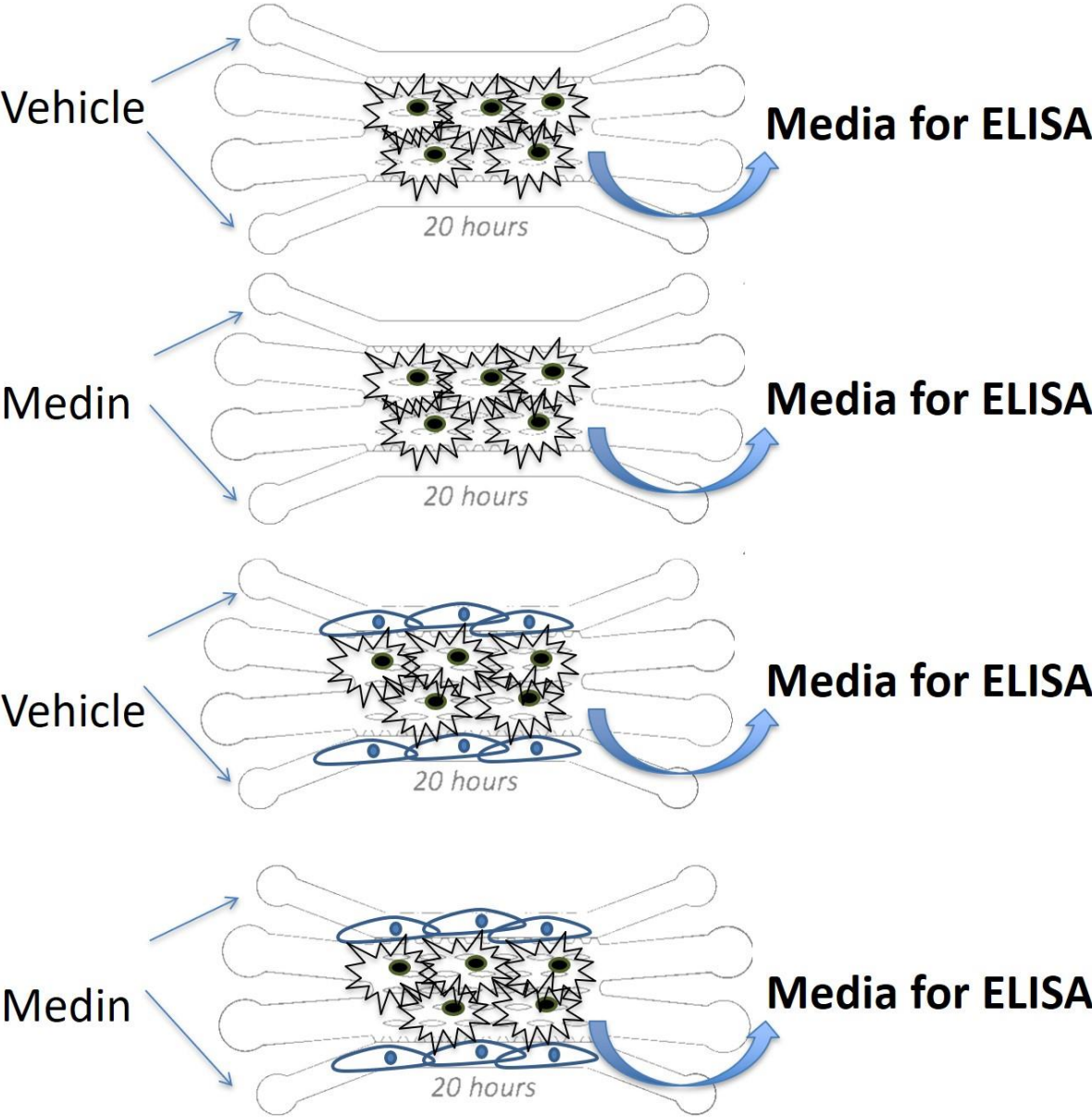


Figure S3. Immune activation by medin is NF κ B-dependent. A. ECs exposed to medin show increased NF κ B activation (phosphorylated NF κ B) starting at 15 minutes, peaks at 1 hour but persists for 20 hours. B-E. When medin is co-treated with specific NF κ B inhibitor RO106-9920, there was abolition of medin-induced increased gene expression of IL-8, IL-6, ICAM-1 and PAI-1. F-H. RO106-9920 co-treatment with medin did not reverse medin's effect on cellular viability when compared to medin alone (B). * $p < 0.05$, ** $p < 0.01$, *** $p < 0.001$. EC-endothelial cell, IL-interleukin, ICAM-1-intercellular adhesion molecule-1, PAI-1-plasminogen activator inhibitor-1, NF κ B-nuclear factor-kappa B, M-medin

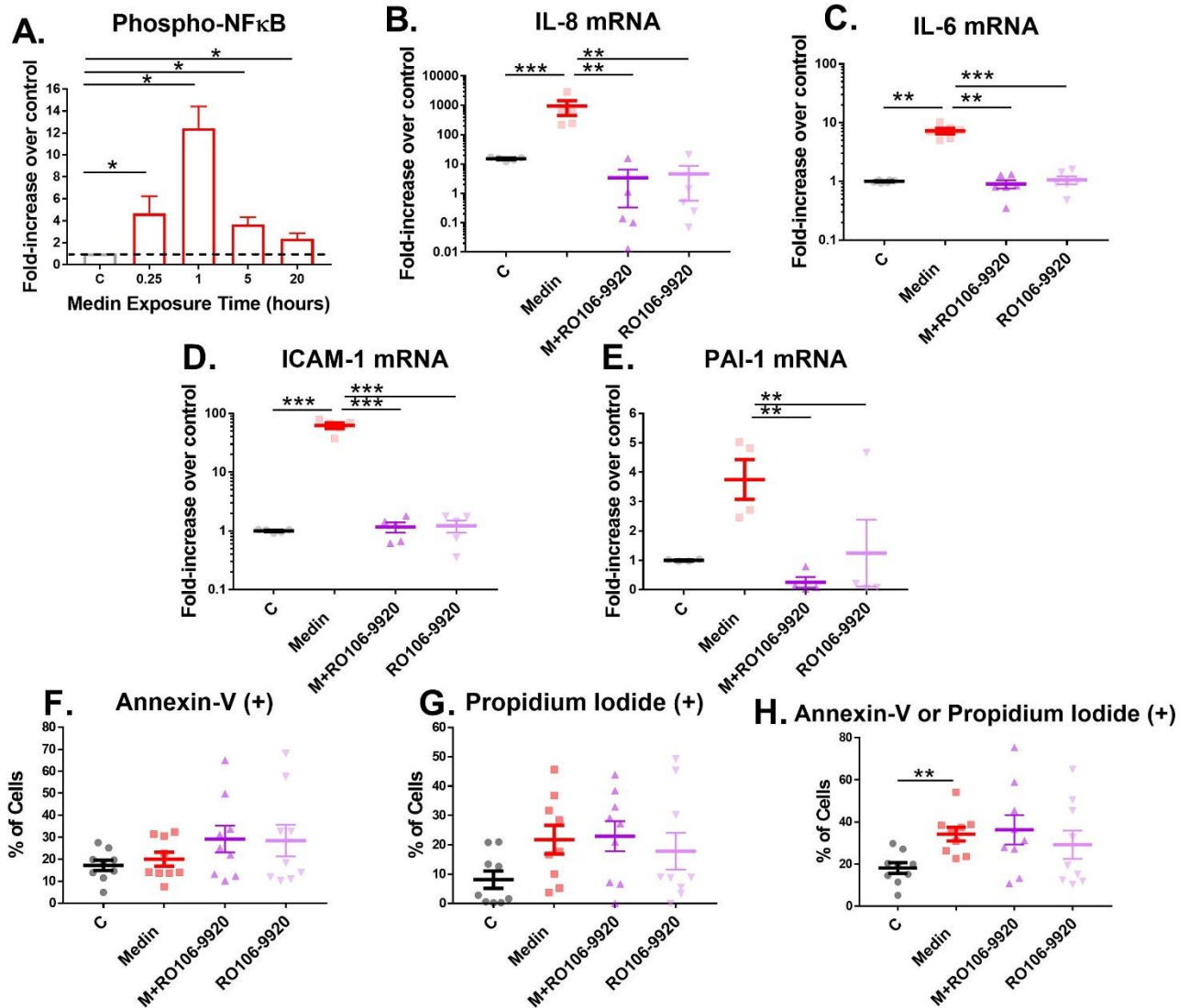


Figure S4. Flow cytometry to assess endothelial cell viability. A. Representative flow cytometry images showing annexin V fluorescence data in X axis and propidium iodide data in y axis from 1 independent experiment. Consolidated data analyses are shown in Figure 3. B-C Histogram profile showing number of cells (y axis) and fluorescence signal (x axis) for propidium iodide (B) and Annexin V (C), presented in relation to control signal. NLGM1-monosialoganglioside nanoliposomes

